Ln Dependence of the Large-Capacity Oxygen Storage/Release Property of Ln Oxysulfate/Oxysulfide Systems

Masato Machida,* Tomoatsu Kawano, Masakazu Eto, Dongjie Zhang, and Keita Ikeue

Department of Nano Science and Technology, Graduate School of Science and Technology, Kumamoto University, 2-39-1 Kurokami, Kumamoto 860-8555, Japan

Received November 3, 2006. Revised Manuscript Received December 7, 2006

In a series of large-capacity oxygen storage materials using the redox between $Ln_2O_2SO_4(S^{6+})$ and $Ln_2O_2S(S^{2-})$, the Pr system can work at as low as 600 °C, compared to ≥650 °C required for Ln = La, Nd, and Sm. The exceptional character of the Pr system has been studied from physicochemical points of view by means of thermogravimetric analysis, X-ray photoelectron spectroscopy, X-ray diffraction, Rietveld analysis, Fourier transform infrared spectroscopy, and Raman spectroscopy. Unlike the other Ln oxysulfates/oxysulfides, the Pr system contained a considerable amount of tetravalent cation (Pr^{4+}) on the surface. The smooth redox between Pr^{3+} and Pr^{4+} would promote the oxidation of bulk Pr_2O_2S to $Pr_2O_2SO_4$. On the other hand, the smooth reduction of $Pr_2O_2SO_4$ to Pr_2O_2S appears to be associated with a local structure of sulfate. The X-ray and spectroscopic analysis predicted that the tetrahedral SO_4 unit of $Pr_2O_2SO_4$ is more distorted than that of $La_2O_2SO_4$. Instability caused by the stronger distortion of SO_4 would lead to the easier reduction to S^{2-} species. A synergy of these two different effects on the redox process of the Pr system seems to be a possible reason for the successful oxygen storage/release cycles at lowest possible temperatures.

Introduction

The oxygen storage and release property has become one of the important functions of the three-way catalysts used for present automotive emission control.[1−3] The most widely used oxygen storage material, CeO_2-ZrO_2, works on the basis of the reversible redox reaction between Ce^{4+} and Ce^{3+}.[4−8] The corresponding oxygen storage capacity (OSC) cannot thus exceed 0.25 mol of $O_2 \cdot mol^{-1}$. By contrast, we have recently reported a much larger OSC of lanthanide oxysulfates/oxysulfides, $Ln_2O_2SO_4/Ln_2O_2S$, which utilizes the nonmetallic element (S) as a redox site instead of Ce.[9−11] The reduction by H_2, CO, or hydrocarbons and subsequent reoxidation by O_2 between $Ln_2O_2SO_4(S^{6+})$ and $Ln_2O_2S(S^{2-})$ achieved the oxygen storage of 2 (mol of O_2)$\cdot mol^{-1}$, which is eight times larger than that of the CeO_2-ZrO_2 system. Nevertheless, because of the higher operation temperature required for $Ln_2O_2SO_4$ compared to the CeO_2-ZrO_2 system, we must study the microstructural as well as chemical modifications. Impregnation of a small amount (1 wt %) of noble metals such as Pd or Pt can promote the reduction as well as reoxidation of $Ln_2O_2SO_4$.[10] Furthermore, porous oxysulfates synthesized by a surfactant-templating route can increase the specific surface area and thus the rate of oxygen storage and release.[11]

A wide variety of Ln^{3+} can form $Ln_2O_2SO_4$ and Ln_2O_2S. Both phases crystallize as a similar structure, which can be described by alternating stacking of a $Ln_2O_2^{2+}$ layer and a layer of anions, SO_4^{2-} or S^{2-}.[12] The phase transformation is therefore regarded as removal or insertion of O^{2-} surrounding sulfur. Actually, however, both thermostability and the redox property of these systems are dependent on Ln elements. Generally, $Ln_2O_2SO_4$ appears as a metastable intermediate phase between $Ln_2(SO_4)_3$ and Ln_2O_3. Cerium does not form a stable oxysulfate phase. The thermal stability of $Ln_2O_2SO_4$ decreased monotonously with an increase of the Ln atomic number, and lanthanides heavier than Sm cannot be used because of the instability at ≥1000 °C.[10] Unlike the thermostability, the Ln dependence of the redox temperature of $Ln_2O_2SO_4/Ln_2O_2S$ is more complicated; that is, among four series of Ln = La, Pr, Sm, and Nd, the Pr system can work at the lowest possible temperature.[10] This exceptional performance of Pr suggests that the character of Ln^{3+} may affect the redox property and a local structure of the sulfate unit.

* To whom correspondence should be addressed. E-mail: machida@chem.kumamoto-u.ac.jp.

(1) Taylar, K. C. Automobile catalytic converters. In *Catalysis−Science and Technology*; Anderson, J. R., Boudart, M., Eds.; Springer-Verlag: Berlin, 1984; Vol. 5.
(2) Bernal, S.; Kaspar, J.; Trovarelli, A. *Catal. Today* **1999**, *2*, 50.
(3) Trovarelli, A. In *Catalysis by ceria and related materials*; Trovarelli, A., Ed.; Imperial College Press: London, 2002; Vol. 2.
(4) Ozawa, M.; Kimura, M.; Isogai, A. *J. Alloys Compd.* **1993**, *193*, 73.
(5) Zamur, F.; Trovarelli, A.; de Leitenburg, C.; Dolcetti, G. *J. Chem. Soc., Chem. Commun.* **1995**, 965.
(6) Balducci, G.; Fornasiero, P.; Di Monte, R.; Kaspar, J.; Meriani, S.; Graziani, M. *Catal. Lett.* **1995**, *33*, 193.
(7) Kaspar, J.; Fornasiero, P. *J. Solid State Chem.* **2003**, *171*, 19.
(8) Pijolat, M.; Prin, M.; Soustelle, M.; Touret, O.; Nortier, P. *J. Chem. Soc., Faraday Trans.* **1995**, *91*, 3941.
(9) Machida, M.; Kawamura, K.; Ito, K. *Chem. Commun.* **2004**, 662.
(10) Machida, M.; Kawamura, K.; Ito, K.; Ikeue, K. *Chem. Mater.* **2005**, *17*, 1487.
(11) Machida, M.; Kawamura, K.; Kawano, T.; Zhang, D.; Ikeue, K. *J. Mater. Chem.* **2006**, *16*, 3084.
(12) Zhukov, S.; Yatsenko, A.; Chernyshev, V.; Trunov, V.; Tserkovnaya, E.; Anston, O.; Hosla, J.; Baules, P.; Schenk, H. *Mater. Res. Bull.* **1997**, *32*, 43.

10.1021/cm062625n CCC: $37.00
Published on Web 01/24/2007

In the present work, physicochemical and structural characterization has been carried out with the aim of elucidating this Ln dependence of oxygen storage. The redox process has been studied by means of thermogravimetric analysis (TGA) and X-ray photoelectron spectroscopy (XPS). A local environment of the active site has been compared for the different Ln^{3+} on the basis of the structural analysis by means of X-ray diffraction (XRD) and IR and Raman spectroscopies.

Experimental Section

A series of lanthanum oxysulfates, $Ln_2O_2SO_4$ (Ln = La, Pr, Nd, and Sm), were synthesized by heating commercial $Ln_2(SO_4)_3 \cdot nH_2O$ (Rare Metallic Co., Ltd.) at 900 °C for 5 h in air. Subsequent heating in a stream of H_2 at 800 °C was conducted to yield corresponding oxysulfides, Ln_2O_2S. Energy dispersive X-ray fluorescence analysis (Horiba MESA-500W) was used to determine the S/Ln ratio. The powder XRD was measured on a Rigaku RINT with monochromated Cu Kα radiation (40 kV, 200 mA) in a step-scan mode over the 2θ range of 10−100° (step size, 0.02°, and counting time, 4 s). The structure analysis was carried out by the Rietveld method using the RIETAN-2000 profile refinement program.[13] The peak shape was described by a pseudo-Voigt function, and the background level was defined by a polynomial function. The scale factor, the counter zero point, the peak asymmetry, and the unit cell dimensions were refined in addition to the atomic parameters. Fitting between calculated and observed data was evaluated in terms of four agreement factors, R_{wp}, R_p, R_I, and R_F.[14]

The XPS spectra were measured on a VG Sigmaprobe spectrometer using Al Kα radiation (15 kV, 7 mA). The binding energy calculation was checked using the line position of C 1s as an internal reference. The charging effect was ruled out in the measurement because the binding energy for C 1s was identical for all of the samples. The normal operating pressure in the analysis chamber was controlled at less than 10^{-6} Pa during the measurement. The Fourier transform infrared (FTIR) spectra were recorded on a Jasco FTIR-610 spectrometer by using a KBr method. Raman spectra were obtained on a Jasco NRS-3100 spectrometer using a 532.1 nm laser as an excitation source. The BET surface area was calculated from N_2 adsorption isotherms measured at 77 K (Belsorp).

The reduction/reoxidation behavior of $Ln_2O_2SO_4$ was analyzed by a microbalance (TGA, Rigaku 8120), which is connected to a controlled gas supplying system. The sample (ca. 10 mg) was heated in a flowing gas mixture of 5% H_2 and He (20 $cm^3 \cdot min^{-1}$) at a constant rate (10 °C·min^{-1}) up to 950 °C. The reduction onset (T_R) and offset (T_R') temperatures were determined from the differential thermogravimetry (DTG) curves as the point at which an extrapolated baseline intersects two tangent lines of a peak as a result of reduction of $Ln_2O_2SO_4$ to Ln_2O_2S. After the measurement, the sample was cooled to ambient temperature in a stream of 5% H_2/He. This is followed by the second heating in a flowing gas mixture of 2.5% O_2/He (20 $cm^3 \cdot min^{-1}$) at a constant rate (10 °C·min^{-1}) up to 950 °C to measure the reoxidation profiles. The reoxidation onset (T_O) and offset (T_O') temperatures were determined from the DTG curves in a similar way.

Dynamic reduction−oxidation cycles of $Ln_2O_2SO_4$ were also studied by the use of the flow microbalance. For this measurement, as-prepared oxysulfates were impregnated with an aqueous solution of palladium nitrate and then calcined at 450 °C to produce Pd-loaded samples (1 wt % loading). The Pd-loaded sample (ca. 10 mg) was first heated in a stream of He up to 700 °C, where the constant weight was attained within 30 min. Then, the gas feed to the sample was switched at constant intervals between 5% H_2 and 20% O_2 balanced by He with recording the sample weight at this temperature.

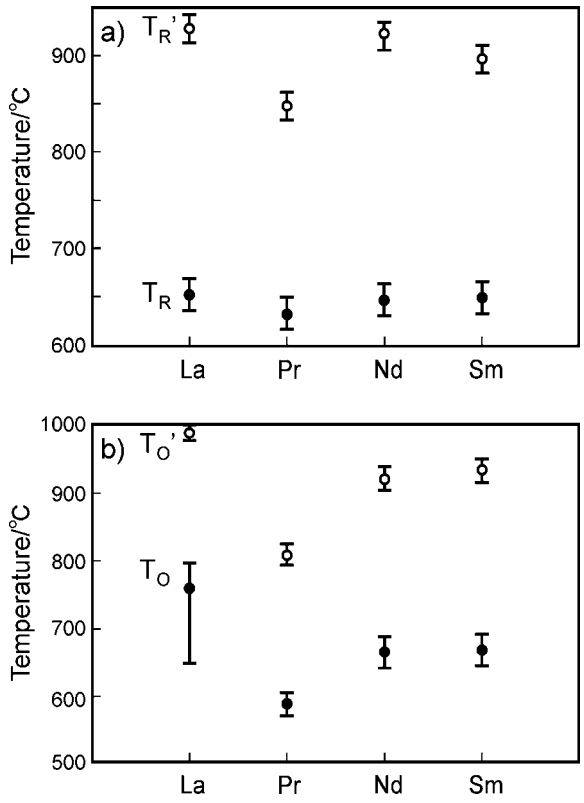

Figure 1. (a) Onset (T_R) and offset (T_R') temperatures for the reduction of $Ln_2O_2SO_4$ to Ln_2O_2S in 5% H_2/He and (b) onset (T_O) and offset (T_O') temperatures for the reoxidation of Ln_2O_2S to $Ln_2O_2SO_4$ in 2.5% O_2/He.

Results and Discussion

Reduction/Reoxidation of $Ln_2O_2SO_4$. Four as-synthesized $Ln_2O_2SO_4$ (Ln = La, Pr, Nd, and Sm) exhibited very similar XRD patterns, which were assigned to a monoclinic phase. Their S/Ln ratios agreed with 0.5 within an experimental error. The BET surface area was in a rage of 5−8 $m^2\ g^{-1}$. To evaluate the Ln dependence of oxygen storage/release properties, the TGA measurement was carried out in a stream of 5% H_2 in He and subsequently in a stream of 2.5% O_2 in He. The OSCs of these compounds measured at 700 °C corresponded to 2 (mol of O_2)·mol^{-1}. Nevertheless, the temperatures where the reduction as well as reoxidation started are dependent on Ln. Figure 1a compares reduction onset (T_R) and offset (T_R') temperatures for four $Ln_2O_2SO_4$. Although both T_R and T_R' of $Pr_2O_2SO_4$ are lower than those of the other three $Ln_2O_2SO_4$, a larger difference in T_R' particularly suggests the higher reduction rate of $Pr_2O_2SO_4$. A more obvious Ln dependence was observed in the reoxidation to $Ln_2O_2SO_4$ as shown in Figure 1b. The Pr system exhibited T_O lower than T_R, whereas the others (La, Nd, and Sm) showed T_O almost equal to or higher than T_R. The Pr system can thus facilitate not only the reduction of oxysulfate but also, more significantly, the reoxidation at as

(13) Izumi, F.; Ikeda, T. *Mater. Sci. Forum* **2000**, *321, 198.*
(14) Young, R. A. In *The Rietveld Method*; Young, R. A., Ed.; Oxford University Press: Oxford, 1993; Chapter 1.

Table 1. Weight Changes of $Ln_2O_2SO_4$ (Ln = La and Pr)

	calculated[a]	observed[b]
	Reduction	
La	−15.8%	−15.9%
Pr	−15.6%	−15.6%
	Reoxidation	
La	+18.7%	+17.3%
Pr	+18.5%	+17.4%

[a] Calculated assuming the redox between $Ln_2O_2SO_4$ and Ln_2O_2S. [b] Determined by TGA.

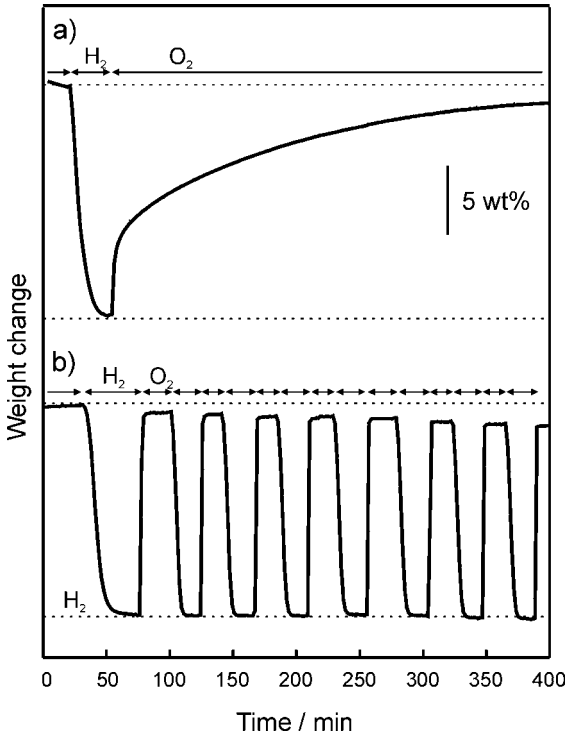

Figure 2. Isothermal reduction−reoxidation cycles at 700 °C over (a) 1 wt % $Pd/La_2O_2SO_4$ and (b) 1 wt % $Pd/Pr_2O_2SO_4$ measured in a microbalance. A mixture of 5% H_2 in He was used for reduction, and a mixture of 20% O_2 in He was used for oxidation.

low as 600 °C, whereas other systems require the heating at ≥650 °C. Calculated and observed weight changes in the reduction/reoxidation of $Ln_2O_2SO_4$ (Ln = La and Pr) are compared in Table 1. In both systems, the weight changes observed by TGA measurement agreed with those calculated assuming the reversible redox between sulfate (SO_4^{2-}) and sulfide (S^{2-}). It can therefore be concluded that the oxygen storage in these systems is attributed only to the redox of sulfur species.

To increase the rate of redox between oxysulfate and oxysulfide, impregnation of noble metals is a promising modification, because spillover of chemisorbed species can supply active hydrogen as well as oxygen onto the surface of $Ln_2O_2SO_4/Ln_2O_2S$.[10] Figure 2 displays the dynamic oxygen release/storage cycles of 1 wt % Pd-loaded $La_2O_2SO_4$ and $Pr_2O_2SO_4$ measured in a flow microbalance at 700 °C. On approaching a constant weight in flowing He at 700 °C, the gas feed was switched between 5% H_2 in He and 20% O_2 in He. The reduction of $La_2O_2SO_4$ in 5% H_2 was completed within approximately 1 h, but the subsequent reoxidation in 20% O_2 took more than 6 h (a). By contrast, the reduction as well as reoxidation of $Pr_2O_2SO_4$ was so fast

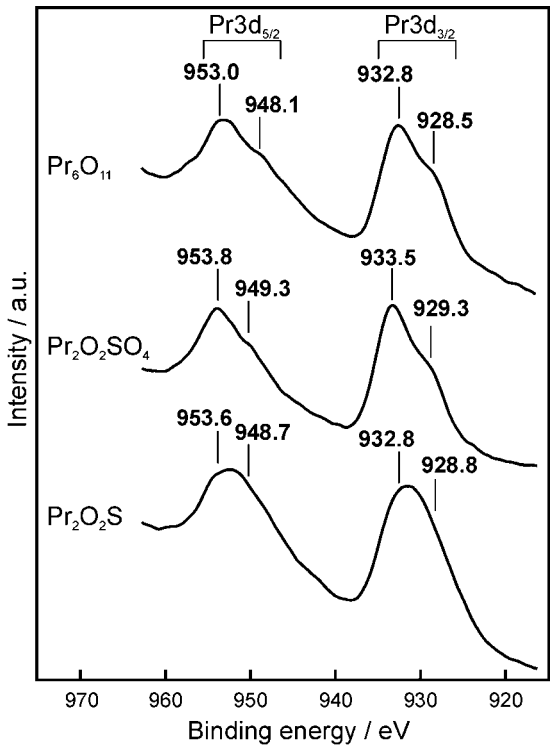

Figure 3. Pr 3d XPS spectra of Pr_6O_{11}, $Pr_2O_2SO_4$, and Pr_2O_2S.

that the weight changes were completed within approximately 15 min, yielding almost reversible cyclic change of the weight (b). The difference between $La_2O_2SO_4$ and $Pr_2O_2SO_4$ is found to be more obvious in the reoxidation steps as is consistent with Figure 1. The dynamic oxygen release/storage cycles of the Nd and Sm systems were rather similar to that of the La system. Therefore, the following characterization was mainly focused on the comparison between the Pr and the La systems.

Effect of Surface Oxidation State. Because $Ln_2O_2SO_4$ (Ln = La, Pr, Nd, and Sm) phases are stoichiometric and isomorphous, the formal charge on Ln should commonly be 3+. Similarly, a series of Ln_2O_2S compounds should contain Ln in the 3+ oxidation state. This was supported by the fact that the Ln 3d XPS signals of La, Nd, and Sm phases exhibited sole species ascribable to Ln^{3+}. However, this is not the case for Ln = Pr as shown in Figure 3, where peaks due to Pr $3d_{5/2}$ and Pr $3d_{3/2}$ for $Pr_2O_2SO_4$ can be decomposed into two components, 953.8/949.3 eV and 933.5/929.3 eV, respectively. Judging from a simple comparison with a spectrum of Pr_6O_{11}, these signals at lower binding energies agreed with Pr^{3+}, whereas those at higher energies was assigned to Pr^{4+}.[15] The Pr^{4+} species were also detected on Pr_2O_2S, which was synthesized by heating $Pr_2O_2SO_4$ in a stream of H_2. These results suggest that the surfaces of $Pr_2O_2SO_4$ as well as Pr_2O_2S are easily oxidized to yield a considerable amount of Pr^{4+}. On the basis of the intensity of each XPS signals, the fraction of Pr^{4+} was calculated to be 64% for $Pr_2O_2SO_4$ and 50% for Pr_2O_2S. However, the concentration of Pr^{4+} should be negligible when all of the bulk Pr is taken into consideration, because the TGA results

(15) Narula, C. K.; Haack, L. P.; Chun, W.; Jen, H. W.; Graham, G. W. *J. Phys. Chem. B* **1999**, *103*, 3634.

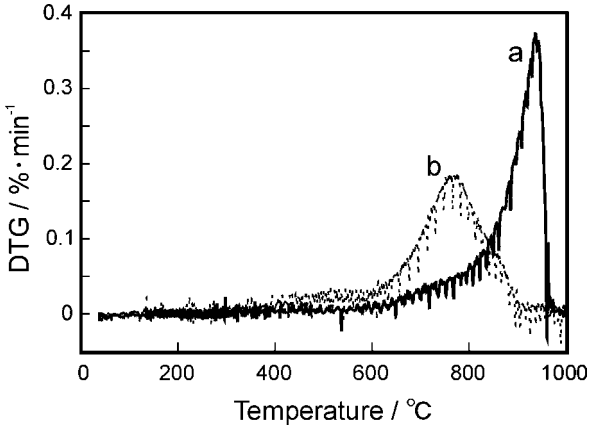

Figure 4. DTG curves of (a) La_2O_2S and (b) 10 wt % Pr_6O_{11}/La_2O_2S measured in 2.5% O_2/He. Heating rate: 10 °C·min^{-1}.

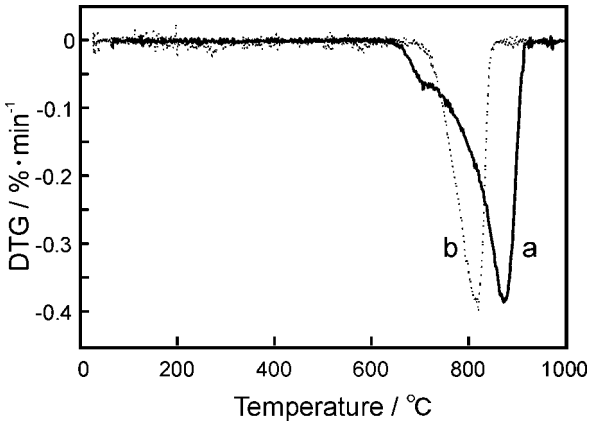

Figure 5. DTG curves of (a) $La_2O_2SO_4$ and (b) 10 wt % $Pr_6O_{11}/La_2O_2SO_4$ measured in 5% H_2/He. Heating rate: 10 °C·min^{-1}.

in Table 1 proved that oxygen storage in the present system is determined only by sulfur redox.

It is assumed that the redox of Pr on the surface would affect the reduction/reoxidation of bulk oxysulfate. As a result of charge compensation accompanied by the creation of Pr^{4+}, oxygen would be adsorbed as negatively charged species onto the surface and may thus promote the oxidation of S^{2-} to SO_4^{2-}. In order to demonstrate these situations, the TGA measurement was conducted for La_2O_2S with and without addition of 10 wt % Pr_6O_{11}. Because of low amount of Pr_6O_{11} loading and its small weight change (less than 0.3% of the total weight), the TGA data will not be affected by the redox of Pr_6O_{11} itself. Figure 4 compares the DTG curves for the oxidation of La_2O_2S and 10 wt % Pr_6O_{11}/La_2O_2S in flowing 10% O_2/He. The weight gain caused by the oxidation of La_2O_2S started at approximately 600 °C, and the maximum rate of the weight gain was observed at approximately 930 °C. However, the addition of Pr_6O_{11} exhibited the maximum rate of oxidation approximately 150 °C lower than in the case of La_2O_2S alone. We also carried out the TGA measurement of $La_2O_2SO_4$ and 10% $Pr_6O_{11}/La_2O_2SO_4$ in a stream of 5% H_2/He (Figure 5), which also suggests the increased rate of reduction of $La_2O_2SO_4$. When Pr_6O_{11} alone was reduced in a similar way, the reduction of Pr^{4+} to Pr^{3+} occurred at 400 °C, which is lower than the temperature for the redox of oxysulfate. Pr^{3+} thus formed can promote the reduction of SO_4^{2-} to S^{2-}, and in a similar way, Pr^{4+} can promote the reoxidation of S^{2-} to SO_4^{2-}. These results may

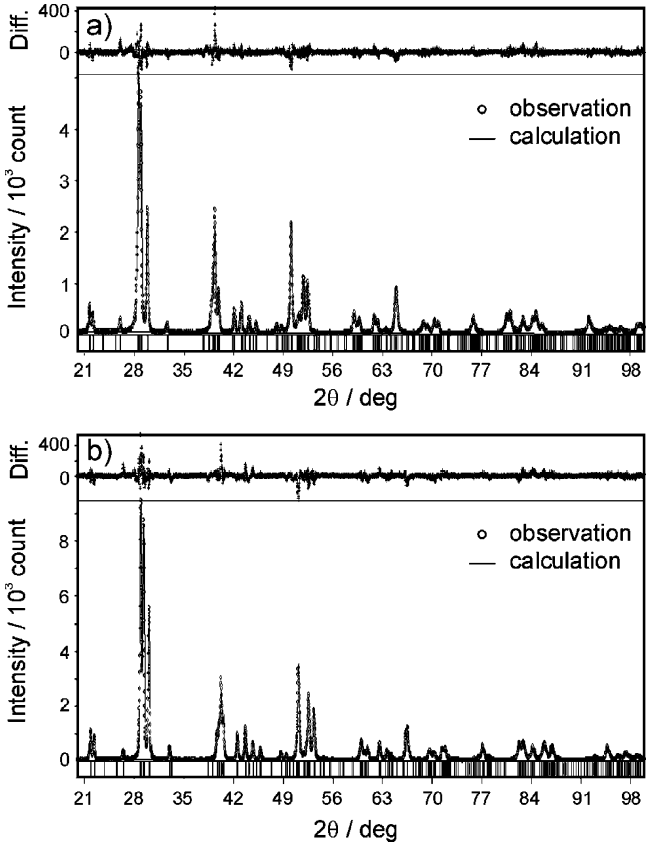

Figure 6. Rietveld X-ray powder pattern fitting for (a) $La_2O_2SO_4$ and (b) $Pr_2O_2SO_4$. The difference between the calculated and observed patterns is shown on the top. The bottom bands display Bragg reflections.

imply that the redox between Pr^{3+} and Pr^{4+} on the surface should play a key role as a mediator for the reduction/reoxidation between S^{2-} and SO_4^{2-} in the Pr system.

Effect of Crystal Structure. Since there is no report so far for the refined structural parameters of $Pr_2O_2SO_4$, we have next carried out the comparative X-ray Rietveld analysis of $La_2O_2SO_4$ and $Pr_2O_2SO_4$. The powder XRD patterns of La and Pr oxysulfates were very similar and indexed with a monoclinic structure with the *C*2/*c* (No. 15) space group. The Rietveld analysis of $La_2O_2SO_4$ was carried out by using the crystallographic data reported by Zhukov et al.[12] as an initial structural model, which gave agreement factors of $R_{wp} = 10.2\%$, $R_p = 7.3\%$, and $R_I = 2.6\%$ with refined structural parameters close to the initial parameters. The obtained structural parameters are subsequently used as an initial structure model for the refinement of $Pr_2O_2SO_4$. The observed, calculated, and difference diffraction profiles are shown in Figure 6. The calculation gave rise to a good fitting with the observed diffraction profile and agreement factors $R_{wp} = 9.2\%$, $R_p = 6.2\%$, and $R_I = 2.9\%$. The refined structural parameters and interactomic distances and angles are listed in Tables 2 and 3, respectively.

The crystal structure of La and Pr oxysulfates can commonly be described by alternating stacking of a layer of sulfate (SO_4^{2-}) and a $Ln_2O_2^{2+}$ layer along the *a*-axis as shown in Figure 7. The $Ln_2O_2^{2+}$ layer consists of LnO_4 tetrahedra linked together by sharing of edges.[12] The lattice parameters, *a*, *b*, and *c*, of $Pr_2O_2SO_4$ are smaller than those of $La_2O_2SO_4$ (Table 2) because of the so-called contraction of lanthanide cations (Ln^{3+}). The O2 in the each SO_4 unit is

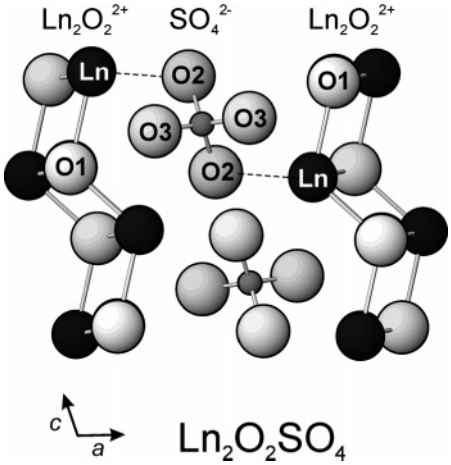

Figure 7. Crystal structure of $Ln_2O_2SO_4$.

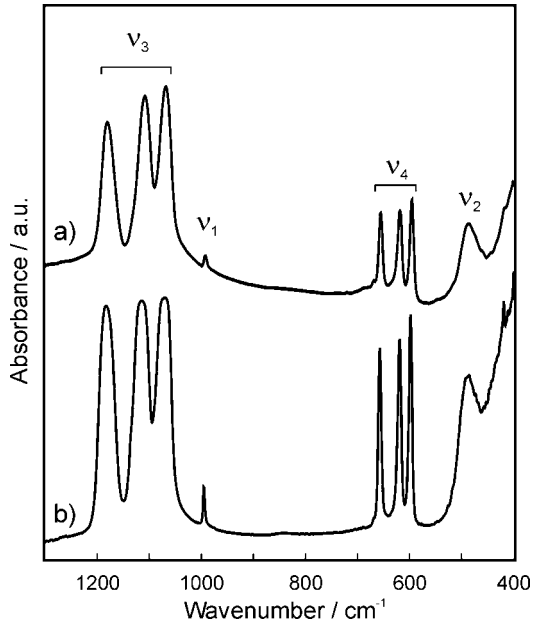

Figure 8. FTIR spectra of (a) $La_2O_2SO_4$ and (b) $Pr_2O_2SO_4$.

coordinated with a Ln atom. The Ln−O1 distances and Ln−O1−Ln angles in the Ln_2O_2 layer are similar and consistent with a smaller ionic radius of Pr^{3+} (Table 3). By contrast, the anion layer of $La_2O_2SO_4$ contains S−O2 (0.158 nm) longer than S−O3 (0.143 nm), whereas La−O2 (0.260 nm) is shorter than La−O3 (0.267 nm). This corresponds to four different O−S−O angles of the range 104−114°. Such a distortion from T_d symmetry is indicative of the bridged bidentate-type coordination of SO_4 to La^{3+} as shown in Figure 7. It should be noted that $Pr_2O_2SO_4$ showed a more obvious difference in S−O distances (0.156 and 0.133 nm) and O−S−O angles (103−116°). These results may suggest a more distorted structure of the SO_4 tetrahedral unit in $Pr_2O_2SO_4$ rather than $La_2O_2SO_4$. Detailed discussion may require the structure refinement by means of neutron diffraction, which is now under investigation. However, the present structural refinement is consistent with the following spectroscopic characterization of sulfate groups. The structural refinements of reduced forms, La_2O_2S and Pr_2O_2S, were also studied in a similar way, but the observed difference was as expected from the ionic radii of La and Pr.

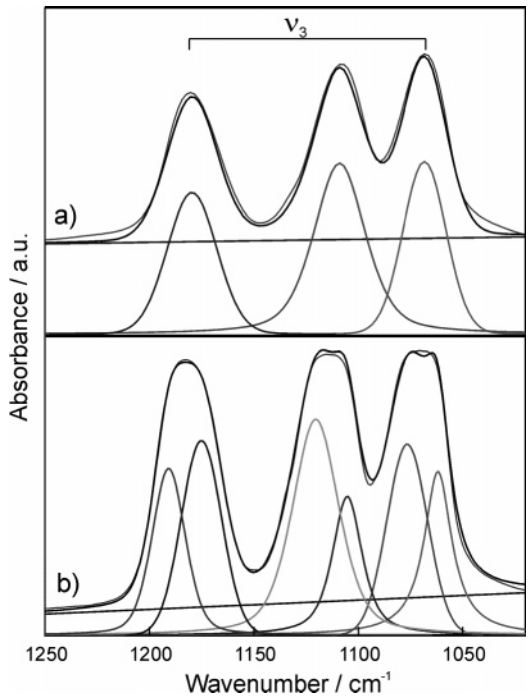

Figure 9. Fitting of SO_4 ν_3 mode FTIR peaks for (a) $La_2O_2SO_4$ and (b) $Pr_2O_2SO_4$.

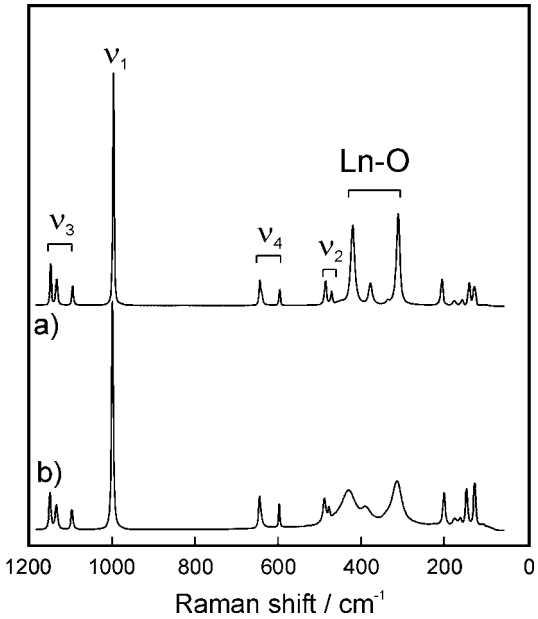

Figure 10. Raman spectra of (a) $La_2O_2SO_4$ and (b) $Pr_2O_2SO_4$.

Effect of Sulfate Structure. Because X-ray structural analysis implied one important structural difference in the tetrahedral sulfate units, the chemical structure of oxysulfate was next studied by means of IR and Raman spectroscopy. Figure 8 shows the IR spectra of $La_2O_2SO_4$ and $Pr_2O_2SO_4$. The four fundamental modes (ν_1, ν_2, ν_3, and ν_4) of a free SO_4^{2-} ion with the T_d point group are Raman active, whereas only ν_3 and ν_4 modes are IR active.[16−18] Actually, however, the IR-inactive modes (ν_1 and ν_2) appeared in the FTIR

(16) Nakamoto, K. *Infrared and Raman Spectra of Inorganic and Coordination Compounds*, 4th ed.; Wiley: New York, 1986.
(17) Mahadevan Pillai, V. P.; Nayar, V. U.; Jordanovska, V. B. *Spectrochim. Acta, Part A* **2000**, *56*, 887.
(18) Georgiev, M.; Wildner, M.; Stoilova, D.; Karadjova, V. *J. Mol. Struct.* **2005**, *753*, 104.

Table 2. Crystallographic Data of $La_2O_2SO_4$ and $Pr_2O_2SO_4$

	atom	site	*g*	*x*	*y*	*z*	*B* ($\times 10^{-2}$ nm^2)
				$La_2O_2SO_4$			
C2/c (No. 15)	La	8f	1.0000	0.1670(0)	0.5014(6)	0.0848(9)	0.18(2)
$a = 1.4348(1)$ nm	O1	8f	1.0000	0.2449(6)	0.020(4)	0.111(3)	0.2(2)
$b = 0.4286(1)$ nm	S	4e	1.0000	0.0	0.044(1)	0.25	1.3(1)
$c = 0.8388(1)$ nm	O2	8f	1.0000	−0.001(1)	0.267(2)	0.098(1)	0.7(3)
$\beta = 106.94(1)°$	O3	8f	1.0000	0.0867(7)	0.864(3)	0.271(3)	2.9(3)
$R_{wp} = 10.18$, $R_p = 7.25$, $R_I = 2.55$, $R_F = 1.75$							
				$Pr_2O_2SO_4$			
C2/c (No.15)	Pr	8f	1.0000	0.1679(0)	0.5012 (4)	0.0851(7)	0.30(2)
$a = 1.4047(1)$ nm	O1	8f	1.0000	0.2468(5)	0.022(3)	0.113(3)	0.7(2)
$b = 0.4244(1)$ nm	S	4e	1.0000	0.0	0.040(1)	0.25	1.7(1)
$c = 0.8281(1)$ nm	O2	8f	1.0000	−0.002(1)	0.269(2)	0.101(1)	1.8(3)
$\beta = 107.08(1)°$	O3	8f	1.0000	0.0843(7)	0.874(2)	0.284(5)	5.3(3)
$R_{wp} = 9.18$, $R_p = 6.24$, $R_I = 2.90$, $R_F = 2.20$							

Table 3. Interatomic Distances and Angles

	$La_2O_2SO_4$	$Pr_2O_2SO_4$
Ln−O1, nm	0.247	0.245
	0.249	0.243
	0.232	0.229
	0.235	0.245
Ln−O1−Ln, deg	98.2	97.7
	102.3	102.3
	108.0	107.7
	102.8	102.0
	126.6	126.6
	119.9	121.9
S−O2, nm	0.158	0.156
S−O3, nm	0.143	0.133
O2−S−O3, deg	114.4 ×2	110.1 ×2
	103.7 ×2	108.1 ×2
O2−S−O2, deg	105.7	102.9
O3−S−O3, deg	114.6	116.4

spectra as a consequence of the low site symmetry in the oxysulfate. In addition, the triply degenerated ν_3 and ν_4 modes gave rise to three strong bands at 1060−1180 and 595−655 cm^{-1}, respectively, suggesting a lowering of symmetry from T_d to C_{2v}. This is consistent with the bridged bidentate-type coordination of SO_4^{2-} as was predicted from the X-ray structural analysis (Table 3 and Figure 7). Although the spectra of these two compounds are similar, $Pr_2O_2SO_4$ showed the small shift of each mode to higher wavenumbers compared to $La_2O_2SO_4$. Another point to be noted is that the ν_3 bands of $Pr_2O_2SO_4$ were broadened and each peak could be decomposed into two Gaussian peak components, whereas the peaks of $La_2O_2SO_4$ were fitted by a single Gaussian peak as shown in Figure 9. These results may imply that the tetrahedral SO_4 in $Pr_2O_2SO_4$ is more distorted in accordance with the result of X-ray structural analysis.

Figure 10 compares the corresponding Raman spectra in the same region. It is reported that Raman spectra of materials containing rare elements can often be complicated by Ln luminescence spectra.[20] In the present case using an 532 nm excitation source, traces of Er and Eu could lead to f−f transitions in the region above 1200 cm^{-1}. Thus, we can neglect this effect in the main difference in Figure 10. Both compounds gave a strong single peak at approximately 990 cm^{-1} due to the nondegenerate ν_1 mode, suggesting that these oxysulfates contain a sole SO_4^{2-} species. The positions of this peak, 993 cm^{-1} for Pr and 990 cm^{-1} for La, shifting to higher Raman shifts from free SO_4^{2-} (981 cm^{-1}) also support the distortion of tetrahedral SO_4^{2-}. Similar shifts were observed for all of the fundamental SO_4 vibrations (ν_1−ν_4). A more significant difference between the two compounds could be observed for bands in the 250−450 cm^{-1} region, which can be assigned to the La−O fundamental modes.[19] In contrast to sharp peaks observed in $La_2O_2SO_4$, $Pr_2O_2SO_4$ showed less intense and very broad peaks in this region. Because the bond length and angles relevant to the La-O1 and Pr-O1 units (Table 3) are very similar, the deformed peak is not ascribable to the structural distortion of the Ln_2O_2 unit. A more plausible reason is the presence of Pr^{4+} on the surface, which would weaken the resonance in Raman scattering by the Pr^{3+}-O unit.

With all these results taken into consideration, the SO_4 unit of $Pr_2O_2SO_4$ is more distorted from the T_d symmetry. With an increase of the distortion in the tetrahedral SO_4^{2-}, the stability is expected to decrease. This is a possible structural reason for the lower reduction temperature of oxygen release from $Pr_2O_2SO_4$. One may point out that a larger distortion may also be unfavorable for the reoxidation of Pr_2O_2S to $Pr_2O_2SO_4$. However, the driving force can be compensated by a large free energy arising from the oxidation of S^{2-} to SO_4^{2-}. From the present results, we expected that the oxygen storage/release of lanthanide oxysulfates can be accelerated by introducing (i) redox species and/or (ii) ions which cause the distortion of the SO_4^{2-} unit. A further structural modification on these aspects is now studied with the aim of increasing the rate of oxygen storage/release of $Pr_2O_2SO_4$.

One of possible applications of the material is its incorporation into the formulation of automotive catalysts. Praseodymium is a high cost and less-abundant resource compared to Ce, which will be the main drawback of the present system, but the effect of the large-capacity oxygen storage on the catalytic performance is of great interest to not only the industrial but also the scientific points of view. More studies are also concentrated on designing the catalysts and characterizing their performance under dynamic feed stream conditions.

Concluding Remarks

Among a series of Ln oxysulfate (Ln = La, Pr, Nd, and Sm), the Pr compound exhibited the redox cycles at the

(19) Cornaglia, L. M.; Múnera, J.; Irusta, S.; Lombardo, E. A. *Appl. Catal., A* **2004**, *263*, 91.
(20) Fornasiero, P.; Speghini, A.; Di Monte, R.; Bettinelli, M.; Kapar, J.; Bigotto, A.; Sergo, V.; Graziani, M. *Chem. Mater.* **2004**, *16*, 1938.

lowest temperature. The oxidation from oxysulfide to oxysulfate is thermodynamically favorable in the presence of O_2 and is significantly promoted by the redox of Pr^{3+}/Pr^{4+} on the surface of Pr_2O_2S. The Pr^{4+} species on the surface play a role of mediator for the oxidation of S^{2-} to SO_4^{2-}. Although Ce and Tb also can take both tetravalent and trivalent states, these lanthanides cannot form thermally stable oxysulfates. Ease of the sulfate reduction seems to be consistent with the structural distortion of an SO_4^{2-} unit in the oxysulfate. The distortion from the T_d symmetry is largest for the Pr compound, the sulfate of which should therefore be most unstable for the reduction to oxysulfide.

Acknowledgment. This study was supported by Industrial Technology Research Grant Program in '05 from New Energy and Industrial Technology Development Organization (NEDO) of Japan, a Grant-in-Aid for Scientific Research on Priority Area (440) from the Ministry of Education, Culture, Sports, Science and Technology (MEXT), and Nippon Sheet Glass Foundation for Materials Science and Engineering.

CM062625N